



# Spinal cord astroblastoma with *EWSR1-BEND2* fusion classified as HGNET-*MN1* by methylation classification: a case report

Takeyoshi Tsutsui<sup>1</sup> · Yoshiki Arakawa<sup>1</sup> · Yasuhide Makino<sup>1</sup> · Hiroharu Kataoka<sup>1</sup> · Yohei Mineharu<sup>1</sup> · Kentaro Naito<sup>2</sup> · Sachiko Minamiguchi<sup>3</sup> · Takanori Hirose<sup>4</sup> · Sumihito Nobusawa<sup>5</sup> · Yoshiko Nakano<sup>6</sup> · Koichi Ichimura<sup>6</sup> · Hironori Haga<sup>3</sup> · Susumu Miyamoto<sup>1</sup>

Received: 24 April 2021 / Accepted: 15 July 2021 / Published online: 27 July 2021  
© The Japan Society of Brain Tumor Pathology 2021

## Abstract

The most recurrent fusion of central nervous system high-grade neuroepithelial tumor with *MN1* alteration (HGNET-*MN1*) is *MN1* rearrangement. Here, we report the case of a 36-year-old man with spinal cord astroblastoma showing *Ewing Sarcoma breakpoint region 1/EWS RNA-binding protein 1 (EWSR1)-BEN domain-containing 2 (BEND2)* fusion. The patient presented with back pain, gait disturbance and dysesthesia in the lower extremities and trunk. Magnetic resonance imaging showed an intramedullary tumor at the T3–5 level, displaying homogeneous gadolinium enhancement. Partial tumor removal was performed with laminectomy. Histological examinations demonstrated solid growth of epithelioid tumor cells showing high cellularity, a pseudopapillary structure, intervening hyalinized fibrous stroma, and some mitoses. Astroblastoma was diagnosed, classified as HGNET-*MN1* by the German Cancer Research Center methylation classifier. *MN1* alteration was not detected by fluorescence in situ hybridization (FISH), but *EWSR1-BEND2* fusion was detected by FISH and RNA sequencing. Previously, a child with *EWSR1-BEND2* fusion-positive spinal astroblastoma classified as HGNET-*MN1* was reported. In conjunction with that, the present case provides evidence that *EWSR1-BEND2* fusion is identified in the entity of HGNET-*MN1*. Taken together, the *BEND2* alteration rather than *MN1* may determine the biology of a subset of the central nervous system HGNET-*MN1* subclass.

**Keywords** Astroblastoma · CNS high-grade neuroepithelial tumor with *MN1* alteration (HGNET-*MN1*) · Ewing Sarcoma breakpoint region 1/EWS RNA-binding protein 1 (*EWSR1*) · BEN domain-containing 2 (*BEND2*) · *EWSR1-BEND2* fusion

## Abbreviations

HGNET-MN1	CNS high-grade neuroepithelial tumor with MN1 alteration
EWSR1	Ewing Sarcoma breakpoint region 1/EWS RNA-binding protein 1
BEND2	BEN domain-containing 2
DKFZ	The German Cancer Research Center
FISH	Fluorescence in situ hybridization
CNS-PNETs	Primitive neuroectodermal tumors of the central nervous system

✉ Yoshiki Arakawa  
yarakawa@kuhp.kyoto-u.ac.jp

<sup>1</sup> Department of Neurosurgery, Kyoto University Graduate School of Medicine, 54 Kawahara-cho Shogoin Sakyo-ku, Kyoto 606-8507, Japan

<sup>2</sup> Department of Neurosurgery, Osaka City University Graduate School of Medicine, Osaka 545-8585, Japan

<sup>3</sup> Department of Diagnostic Pathology, Kyoto University Graduate School of Medicine, Kyoto 606-8507, Japan

<sup>4</sup> Department of Diagnostic Pathology, Hyogo Cancer Center, Akashi, Hyogo 673-8558, Japan

<sup>5</sup> Department of Human Pathology, Gunma University Graduate School of Medicine, Gunma 371-8514, Japan

<sup>6</sup> Division of Brain Tumor Translational Research, National Cancer Center Research Institute, Tokyo 104-0045, Japan

## Introduction

Astroblastomas are rare neuroepithelial tumors of unknown origin [1, 2], arising mostly in the cerebrum and rarely in the spinal cord. These tumors most often occur in the first to fourth decades of life, and show a female predominance [1, 2]. Although their status as a pathological entity has

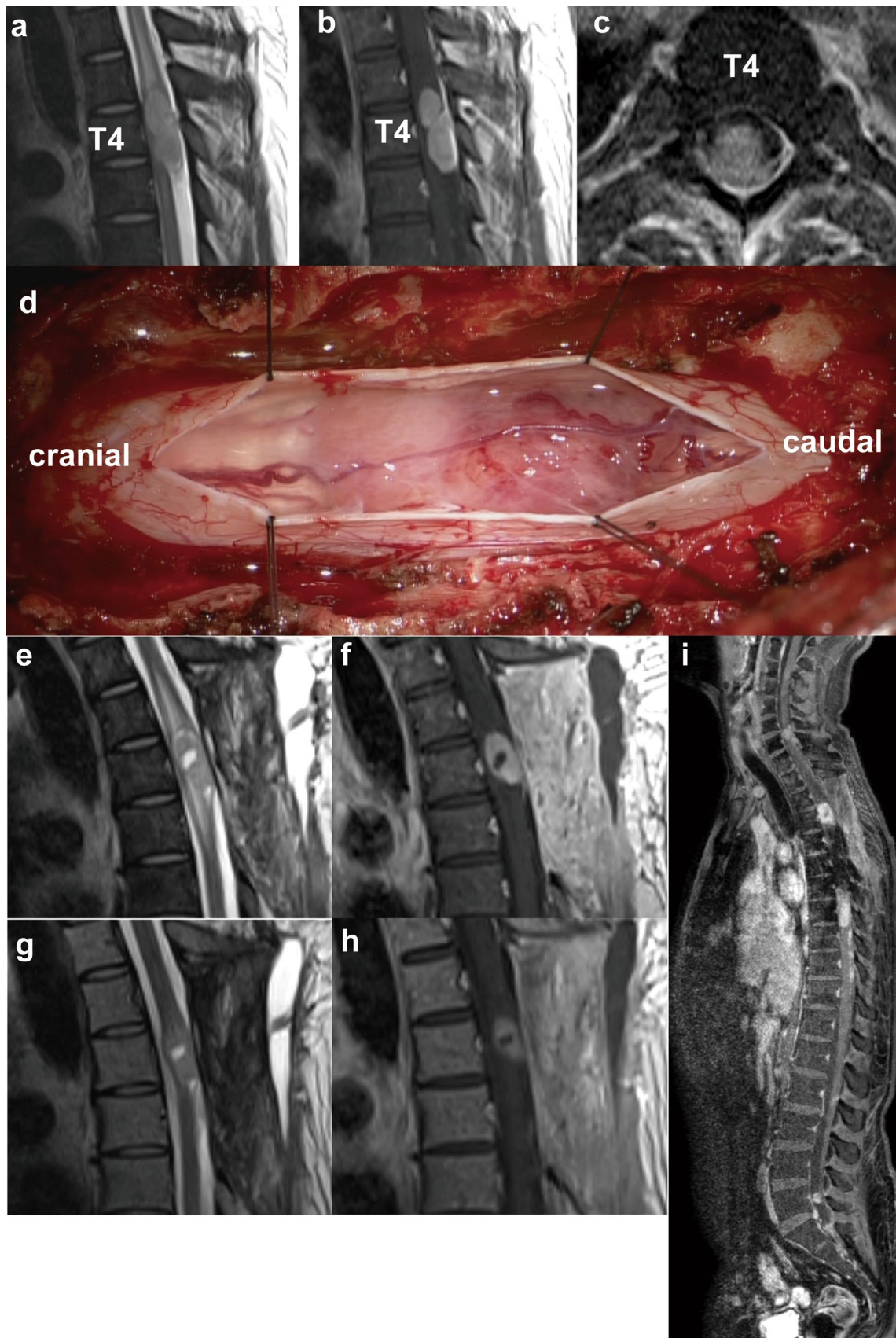


**Fig. 1** Sequential MRI at initial diagnosis and after partial tumor resection. **a–c** An intra-axial tumor is identified at the T3–5 level. T2-weighted imaging demonstrates peritumoral edema in the spinal cord (**a**). The tumor shows homogeneous enhancement (**b, c**). **d** Intraoperative view of the tumor. An exophytic tumor is observed at the T4 level, showing grayish coloration. **e–f** At 1 month postoperatively, residual tumor at the T4 level shows rapid growth and perifocal edema extending downward to the C5 level (**e**). Gadolinium-enhanced T1-weighted imaging shows necrotic changes at the center of the tumor (**f**). **g–h** In late phase of radiotherapy concomitant with chemotherapy using temozolomide and bevacizumab, perifocal edema resolves (**g**) in association with a reduction in tumor size (**h**). Massive dissemination of the tumor was identified 12 months after chemoradiotherapy (**i**)

not been fully determined, the genetic architecture of these tumors has gradually been elucidated.

In 2016, genome-wide DNA methylation analyses of primitive neuroectodermal tumors of the central nervous system (CNS-PNETs) identified four new molecular entities, and one new entity termed CNS high-grade neuroepithelial tumor with MN1 alteration (HGNET-*MN1*) was over-represented by astroblastoma [3]. Similarly, around half of pathologically diagnosed astroblastomas were classified as CNS HGNET-*MN1* [4]. This group has been characterized by *MN1* (22q12.3) rearrangement, in which BEN domain-containing 2 (*BEND2*; Xp22.13) and CXXC-type zinc-finger protein 5 (*CXXC5*; 5q31.2) are the main fusion partners of the *MN1* gene [3]. In 2020, our research group reported the case of a 3-month-old boy with spinal astroblastoma, classified as CNS HGNET-*MN1* by the German Cancer Research Center (DKFZ) methylation classification [5, 6] but lacking *MN1* rearrangement. The tumor instead showed gene fusion between *Ewing sarcoma breakpoint region 1/EWS RNA-binding protein 1* (*EWSR1*) and *BEND2* [6]. Herein, we report the case of another patient with primary spinal astroblastoma showing *EWSR1-BEND2* fusion.

## Clinical summary

A 36-year-old man presenting with back pain, gait disturbance and dysesthesia in the lower extremities and trunk was referred to our institution. Neurological examination demonstrated bilateral dysesthesia below the T10 level and thermal hypoalgesia below the S2 level on the right, accompanied by motor weakness of the lower limbs that required a walking aid. Magnetic resonance imaging (MRI) showed a well-demarcated intramedullary tumor spreading exophytically at the T3–5 level, displaying hypointensity on T1-weighted imaging, hyperintensity on T2-weighted imaging, and homogeneous gadolinium enhancement (Fig. 1a–c). No lesion was observed in either the cerebrum or cerebellum. In addition,  $^{18}\text{F}$ -fluorodeoxyglucose-positron emission tomography showed no apparent accumulation in the

tumor (data not shown). The patient underwent partial tumor removal via T3–5 laminectomy. The tumor formed a solid extra-axial mass, which looked grayish (Fig. 1d). The exophytic portion was well demarcated and able to be safely peeled off the spinal cord. The intramedullary portion displayed no clear boundary.

Postoperatively, the residual tumor showed rapid growth with necrotic change. Based on the previous report showing that radiotherapy with concomitant chemotherapy was effective, the patient underwent focal irradiation with 54 Gy in 30 fractions along with bevacizumab (10 mg/kg) and temozolomide (75 mg/m<sup>2</sup>). In the late phase of the adjuvant treatment, the tumor reduced in size and perifocal edema was also diminished (Fig. 1e–h). The patient recovered from back pain and started to walk without assistance. However, massive dissemination of the tumor was identified 12 months after chemoradiotherapy (Fig. 1i).

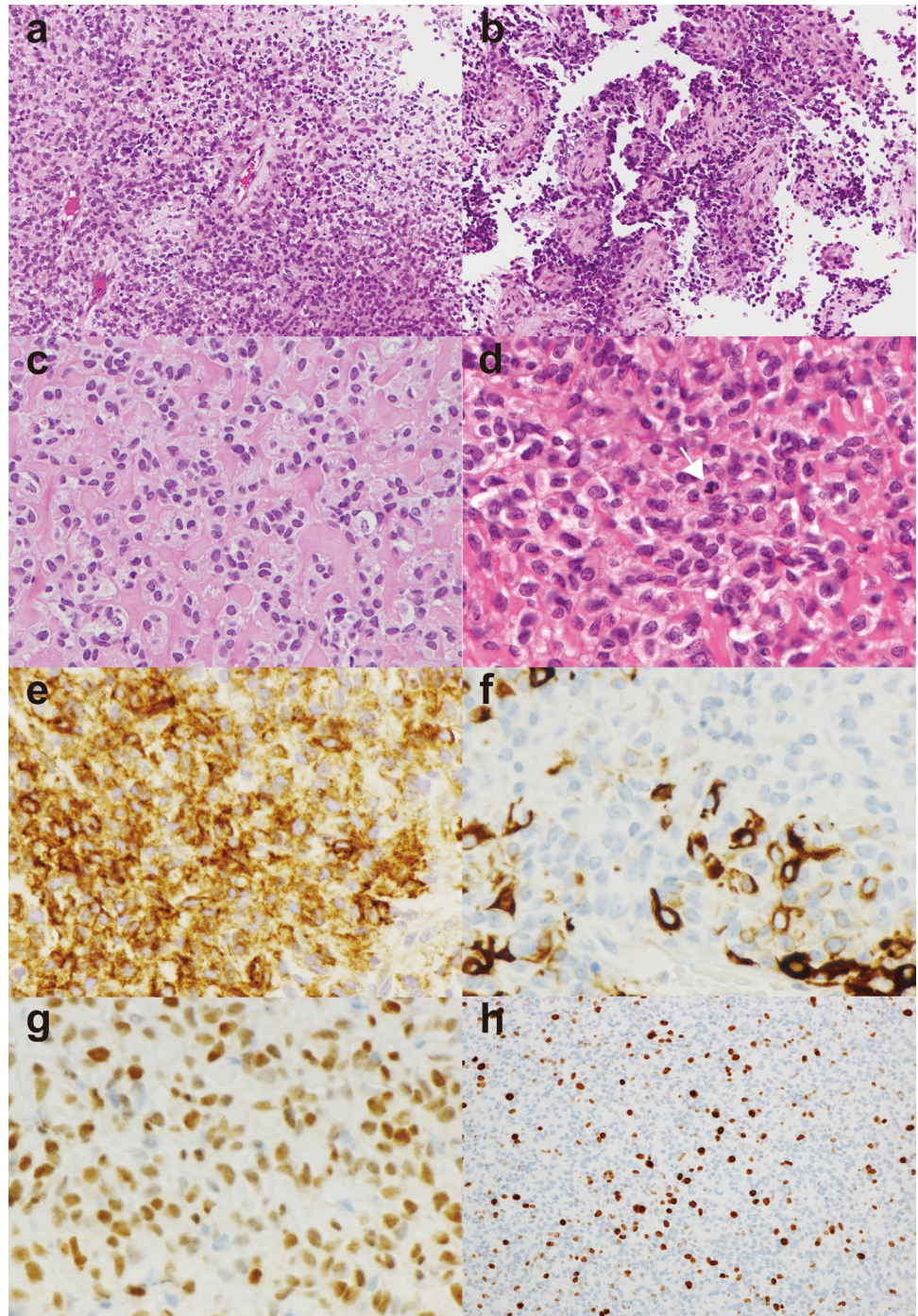
## Pathological findings

Histopathological examination of the tumor tissue showed solid growth of epithelioid tumor cells. A vague perivascular arrangement of tumor cells (Fig. 2a), those in a pseudopapillary pattern (Fig. 2b), and intervening hyalinized fibrous stroma (Fig. 2c) were occasionally observed, but astroblastic pseudorosettes were not discernible. The tumor cells possessed round-to-oval nuclei and relatively abundant eosinophilic cytoplasm with four mitoses per ten high-power fields (Fig. 2d). No necrosis, true rosettes, or calcification was seen. Immunohistochemical analyses showed that tumor cells were strongly and diffusely positive for epithelial membrane antigen (EMA) (Fig. 2e) and focally positive for glial fibrillary acidic protein (GFAP) (Fig. 2f), with nuclear positivity for Olig2 (Fig. 2g) and Ki-67 labeling index 20% (Fig. 2h). Tumor cells were also positive for S-100, but negative for p53, progesterone receptor, and cytokeratin AE1/AE3 (data not shown). A histological diagnosis of astroblastoma was established.

The tumor was classified as HGNET-*MN1* according to the DKFZ methylation classifier [5], with a calibrated score of 0.98. We then analyzed *MN1* and *BEND2* rearrangements by fluorescence in situ hybridization (FISH). No *MN1* rearrangement was detected (Fig. 3a). Due to the previous case of a child showing *EWSR1-BEND2* fusion in astroblastoma, we performed FISH analysis using *EWSR1* and *BEND2* probes. *EWSR1* rearrangement as well as colocalization of *EWSR1* and *BEND2* probes was detected (Fig. 3b, c). Consistent with RNA sequencing and following FISH analysis suggesting *EWSR1-BEND2* fusion, direct sequencing of the cDNA indicated that the breakpoints fell within exon 7 in *EWSR1* and exon 2 in *BEND2*, resulting in an in-frame fusion (Fig. 3d).



**Fig. 2** Histopathological examination of the resected spinal tumor. **a–c** Low magnification ( $\times 10$ ) images with hematoxylin and eosin (HE) staining show perivascular arrangement of tumor cells (**a**) and a pseudo-papillary pattern (**b**). A higher magnification ( $\times 40$ ) images show intervening hyalinized fibrous stroma (**c**), epithelial-like tumor cells with round-to-oval nuclei and eosinophilic cytoplasm and a mitotic figure (white arrow) (**d**). **e–h** Immunohistochemically, tumor cells display strong, diffusely positive staining for EMA (**e**), focally positive staining for GFAP (**f**), and positive nuclear staining for Olig2 (**g**). Ki-67 labeling index is 20% (**h**)



## Discussion

Astroblastoma is a rare and diagnostically challenging glial tumor, accounting for 0.48–2.8% of all gliomas [7]. Astroblastoma occurs mainly in children and young adults. Most astroblastomas occur in the cerebral hemispheres, with the frontal lobe as the most common primary site [8]. Although brainstem and spinal cord origins have been reported on rare occasions [6, 8, 9], most such cases have been reported

recently, probably due to advances in the genetic classification of CNS tumors. The majority of histologically diagnosed astroblastomas have been classified as CNS HGNET-*MNI*, with the remaining classified as pleomorphic xanthoastrocytoma, glioma or ependymoma [10, 11]. Pediatric cerebral astroblastomas that were classified as CNS HGNET-*MNI* were reported to show better prognosis, although the significance of the genetic signature in spinal HGNET-*MNI* remains undetermined [10].

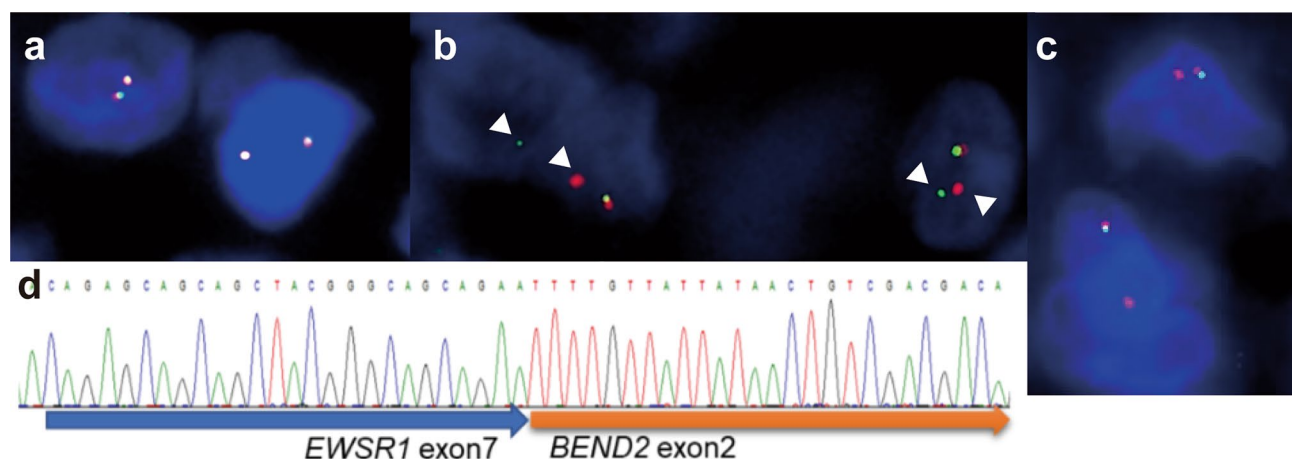


**Fig. 3** Genetic analyses of the resected spinal tumor. **a–c** FISH analysis. No *MN1* rearrangement is identified (**a** red, *MN1* centromeric probe; green, *MN1* telomeric probe). *EWSR1* rearrangement is detected as a split signal with break-apart of two probes for *EWSR1* (**b** arrows; red fluorescence, *EWSR1* centromeric probe; green, *EWSR1* telomeric probe). *EWSR1*-*BEND2* fusion is suggested by

colocalization of the red *EWSR1* centromeric probe and the green *BEND2* probe (**c** red fluorescence, *EWSR1* centromeric probe; green, encompassing the *BEND2* gene). **d** Direct sequence of the cDNA at the break point shows fusion between *EWSR1* exon 7 and *BEND2* exon 2

The first case of primary spinal astroblastoma was reported only recently, by Yamada et al. in 2018 [9]. This may stem from reporting bias: astroblastoma is not usually recognized as a differential diagnosis for spinal cord tumor, and some cases might be misclassified as ependymoma or astrocytoma. Thanks to advances in genetic analyses such as methylation classifier [5], a final diagnosis has become easier to reach with more confidence. Although histologically diagnosed astroblastoma and HGNET-*MN1* may not be identical, molecular classification of HGNET-*MN1* by methylation analysis was compatible with the diagnosis of astroblastoma in the present case. Three cases of spinal astroblastoma have been reported to date, including our own. These three cases are summarized in Table 1 [6, 9]. The tumor was located in the upper cervical spine in one pediatric case and in the upper thoracic spine for the other two tumors in young adults. All three tumors showed an invasive growth pattern despite a well-defined border on MRI examination, and were all treated by partial resection followed by chemoradiotherapy. This treatment showed efficacy in both young adult cases, although the pediatric case proved resistant to the treatment and showed dismal

prognosis. The first case was suggested to show a chromosomal structural abnormality involving the *MN1* gene by FISH. Interestingly, *EWSR1*-*BEND2* fusion without *MN1* rearrangement was detected in two cases, with methylation patterns compatible with CNS HGNET-*MN1* according to the DKFZ classifier. Whether this type of fusion is specific to spinal astroblastoma warrants further investigation. Spinal astroblastoma is an extremely rare tumor, but ependymoma- or anaplastic ependymoma-like tumors or other spinal glial tumors in the spinal region with some unusual findings may be reclassified into astroblastoma if tested by genetic analysis. Thus, previous cases of spinal tumor need to be reviewed, and astroblastoma should be considered among the differential diagnoses for spinal tumors, especially in cases involving children and young adults.

HGNET-*MN1* demonstrates variable morphological and immune-phenotypical features. The characteristic features are astroblastic pseudorosettes and stromal sclerosis [10]. In the present case, only the hyalinized fibrous stroma was identified, while astroblastic pseudorosettes were not well observed [12]. Immunoreactivities for GFAP, S-100

**Table 1** Summary of cases of spinal astroblastoma

Author	Age	Sex	Location	Ki-67	Genetic analysis	Treatment	Postoperative survival
Yamada et al. 2018 [16]	20 years	Female	T1	5%	<i>MN1</i> rearrangement	RT+TMZ+BEV	1 year (alive)
Yamasaki et al. 2020 [17]	3 months	Male	Medulla-C4	34%	<i>EWSR1</i> - <i>BEND2</i> fusion	RT+TMZ+ETP / BEV	30 days (dead)
Present case	36 years	Male	T3-5	20%	<i>EWSR1</i> - <i>BEND2</i> fusion	RT+TMZ+BEV	2 years (alive)

RT radiation therapy, TMZ temozolomide, BEV bevacizumab, ETP etoposide



protein, *Olig2*, and *EMA* were variably demonstrated in *HGNET-MN1* [10, 13].

Only four cases with *EWSR1-BEND2* fusion have been previously reported: one pancreatic neuroendocrine tumor [14], one spinal ependymoma [15], one spinal astroblastoma [6] and the present case. Three of four *EWSR1-BEND2* fusion tumors were localized in the spinal cord. Fusion between *EWSR1* (22q12.2) and partners, i.e., erythroblastosis virus-transforming sequence (avian ETS) transcription factor family, causes various mesenchymal tumors, including Ewing's sarcoma [16]. The N-terminal transcriptional activating domain of *EWSR1* contributes to tumorigenesis. *BEND2* protein is characterized by two BEN domains that bind DNA and are involved in transcription and chromatin regulation [17]. Both domains derived from *EWSR1* and *BEND2* are necessary for tumorigenesis [6]. In addition, in both cases of fusion with *MN1* [18] and *EWSR1* [6], RNA sequencing revealed increased expression of *BEND2* downstream from the breakpoints [3]. This indicates that the fusion of *BEND2* enhances transcription of *BEND2*, which might be associated with oncogenesis. As suggested by a previous report, the presence of *EWSR1-BEND2* fusion tumors could indicate that *BEND2* rather than *MN1* may define the biology of a subset of CNS *HGNET* [6]. Accumulation of case series as well as functional analyses of fusion genes are needed to clarify the pathophysiology of *EWSR1-BEND2*-positive astroblastoma and CNS *HGNET-MN1*.

**Acknowledgements** This study included analysis based upon data generated by the German Cancer Research Center (DKFZ) methylation classifier.

**Author contributions** TT and YA designed the study of the tumor. SM, TH, and H performed histological analyses and diagnosis. SN, YN, and KI performed genetic analyses and data analyses. YM, HK, YM, KN, and SM collected samples. TT and YA wrote the manuscript. All authors read and approved the final manuscript.

**Funding** This work was supported by Grants-in-Aid from the Ministry of Education, Culture, Sports, Science, and Technology, Japan (Grant Nos. 19K09505 and 19K22685).

**Data availability** Not applicable.

## Declarations

**Conflict of interest** The authors declare that they have no competing interests.

**Ethical approval** This report was carried out in accordance with the principles of the Declaration of Helsinki, and approval was obtained from the institutional review boards at Kyoto University Hospital (Approval Number: R1285, R2088).

**Consent for publication** Informed consent was obtained from the patient for publication.

## References

1. Navarro R, Reitman AJ, de Leon GA, Goldman S, Marymont M, Tomita T (2005) Astroblastoma in childhood: pathological and clinical analysis. *Childs Nerv Syst* 21:211–220. <https://doi.org/10.1007/s00381-004-1055-7>
2. Yuzawa S, Nishihara H, Tanino M, Kimura T, Moriya J, Kamoshima Y, Nagashima K, Tanaka S (2016) A case of cerebral astroblastoma with rhabdoid features: a cytological, histological, and immunohistochemical study. *Brain Tumor Pathol* 33:63–70. <https://doi.org/10.1007/s10014-015-0241-5>
3. Sturm D, Orr BA, Toprak UH, Hovestadt V, Jones DTW, Capper D, Sill M, Buchhalter I, Northcott PA, Leis I et al (2016) New brain tumor entities emerge from molecular classification of CNS-PNETs. *Cell* 164:1060–1072. <https://doi.org/10.1016/j.cell.2016.01.015>
4. Lehman NL, Usabalieva A, Lin T, Allen SJ, Tran QT, Mobley BC, McLendon RE, Schniederjan MJ, Georgescu MM, Couce M et al (2019) Genomic analysis demonstrates that histologically-defined astroblastomas are molecularly heterogeneous and that tumors with *MN1* rearrangement exhibit the most favorable prognosis. *Acta Neuropathol Commun*. <https://doi.org/10.1186/s40478-019-0689-3>
5. Capper D, Jones DTW, Sill M, Hovestadt V, Schrimpf D, Sturm D, Koelsche C, Sahm F, Chavez L, Reuss DE et al (2018) DNA methylation-based classification of central nervous system tumours. *Nature*. <https://doi.org/10.1038/nature26000>
6. Yamasaki K, Nakano Y, Nobusawa S, Okuhiro Y, Fukushima H, Inoue T, Murakami C, Hirato J, Kunihiro N, Matsusaka Y et al (2020) Spinal cord astroblastoma with an *EWSR1-BEND2* fusion classified as a high-grade neuroepithelial tumour with *MN1* alteration. *Neuropathol Appl Neurobiol* 46:190–193. <https://doi.org/10.1111/nan.12593>
7. Bhalerao S, Nagarkar R, Adhav A (2019) A case report of high-grade astroblastoma in a young adult. *CNS Oncol*. <https://doi.org/10.2217/cns-2018-0012>
8. Shin SA, Ahn B, Kim SK, Kang HJ, Nobusawa S, Komori T, Park SH (2018) Brainstem astroblastoma with *MN1* translocation. *Neuropathology* 38:631–637. <https://doi.org/10.1111/neup.12514>
9. Yamada SM, Tomita Y, Shibui S, Takahashi M, Kawamoto M, Nobusawa S, Hirato J (2018) Primary spinal cord astroblastoma: case report. *J Neurosurg Spine* 28:642–646. <https://doi.org/10.3171/2017.9.Spine161302>
10. Tauziède-Espariat A, Pages M, Roux A, Siegfried A, Uro-Coste E, Nicaise Y, Sevely A, Gambart M, Boetto S, Dupuy M et al (2019) Pediatric methylation class *HGNET-MN1*: unresolved issues with terminology and grading. *Acta Neuropathol Commun* 7:176. <https://doi.org/10.1186/s40478-019-0834-z>
11. Wood MD, Tihan T, Perry A, Chacko G, Turner C, Pu CF, Payne C, Yu A, Bannykh SI, Solomon DA (2018) Multimodal molecular analysis of astroblastoma enables reclassification of most cases into more specific molecular entities. *Brain Pathol* 28:192–202. <https://doi.org/10.1111/bpa.12561>
12. Lehman NL, Hattab EM, Mobley BC, Usabalieva A, Schniederjan MJ, McLendon RE, Paulus W, Rushing EJ, Georgescu MM, Couce M et al (2017) Morphological and molecular features of astroblastoma, including *BRAFV600E* mutations, suggest an ontological relationship to other cortical-based gliomas of children and young adults. *Neuro Oncol* 19:31–42. <https://doi.org/10.1093/neuonc/now118>
13. Hirose T, Nobusawa S, Sugiyama K, Amatya VJ, Fujimoto N, Sasaki A, Mikami Y, Kakita A, Tanaka S, Yokoo H (2018) Astroblastoma: a distinct tumor entity characterized by alterations of the X chromosome and *MN1* rearrangement. *Brain Pathol* 28:684–694. <https://doi.org/10.1111/bpa.12565>

14. Scarpa A, Chang DK, Nones K, Corbo V, Patch AM, Bailey P, Lawlor RT, Johns AL, Miller DK, Mafficini A et al (2017) Whole-genome landscape of pancreatic neuroendocrine tumours. *Nature* 543:65–71. <https://doi.org/10.1038/nature21063>
15. Ramkissoon SH, Bandopadhyay P, Hwang J, Ramkissoon LA, Greenwald NF, Schumacher SE, O'Rourke R, Pinches N, Ho P, Malkin H et al (2017) Clinical targeted exome-based sequencing in combination with genome-wide copy number profiling: precision medicine analysis of 203 pediatric brain tumors. *Neuro Oncol* 19:986–996. <https://doi.org/10.1093/neuonc/now294>
16. Romeo S, Dei Tos AP (2010) Soft tissue tumors associated with EWSR1 translocation. *Virchows Arch* 456:219–234. <https://doi.org/10.1007/s00428-009-0854-3>
17. Dai Q, Ren AM, Westholm JO, Serganov AA, Patel DJ, Lai EC (2013) The BEN domain is a novel sequence-specific DNA-binding domain conserved in neural transcriptional repressors. *Genes Dev* 27:602–614. <https://doi.org/10.1101/gad.213314.113>
18. Burford A, Mackay A, Popov S, Vinci M, Carvalho D, Clarke M, Izquierdo E, Avery A, Jacques TS, Ingram WJ et al (2018) The ten-year evolutionary trajectory of a highly recurrent paediatric high grade neuroepithelial tumour with MN1:BEND2 fusion. *Sci Rep*. <https://doi.org/10.1038/s41598-018-19389-9>

**Publisher's Note** Springer Nature remains neutral with regard to jurisdictional claims in published maps and institutional affiliations.